Published in final edited form as:
Nat Cell Biol. 2008 April ; 10(4): 489–496. doi:10.1038/ncb1713.

Drosophila STAT is required for directly maintaining HP1 localization and heterochromatin stability

Song Shi[1], **Kimberly Larson**[1], **Dongdong Guo**[1], **Su Jun Lim**[1], **Pranabananda Dutta**[1], **Shian-Jang Yan**[1], and **Willis X. Li**[1,2]

[1] Department of Biomedical Genetics, University of Rochester Medical Center, Rochester, NY 14642, USA.

Abstract

STAT (Signal transducer and activator of transcription) is a potent transcription factor and its aberrant activation by phosphorylation is associated with human cancers[1–4]. We have shown previously that overactivation of JAK, which phosphorylates STAT[5,6], disrupts heterochromatin formation globally in *Drosophila melanogaster*[7]. However, it remains unclear how this effect is mediated and whether STAT is involved. Here, we demonstrate that *Drosophila* STAT (STAT92E) is involved in controlling heterochromatin protein 1 (HP1) distribution and heterochromatin stability. We found, unexpectedly, that loss of STAT92E, had the same effects as overactivation of JAK in disrupting heterochromatin formation and heterochromatic gene silencing, whereas overexpression of STAT92E had the opposite effects. We have further shown that the unphosphorylated or 'transcriptionally inactive' form of STAT92E is localized on heterochromatin in association with HP1, and is required for stabilizing HP1 localization and histone H3 Lys 9 methylation (H3mK9). However, activation by phosphorylation reduces heterochromatin-associated STAT92E, causing HP1 displacement and heterochromatin destabilization. Thus, reducing levels of unphosphorylated STAT92E, either by loss of STAT92E or increased phosphorylation, causes heterochromatin instability. These results suggest that activation of STAT by phosphorylation controls both access to chromatin and activity of the transcription machinery.

To understand the molecular mechanism underlying JAK/STAT-mediated tumour formation, we have previously investigated the role of JAK in a *Drosophila* leukaemia model, in which a hyperactive mutant form of JAK (Tum-1) causes leukaemia-like overproliferation of blood cells[5,8]. We have demonstrated that oncogenic JAK disrupts heterochromatin formation globally, allowing transcriptional activation of genes that are not necessarily direct targets of STAT[7,9]. The molecular mechanism underlying the effects of Hopscotch (Hop, *Drosophila* JAK) on heterochromatin remains unclear. It may be mediated by phosphorylation of STAT92E, as in the canonical JAK/STAT pathway[10,11]. Alternatively, Hop may activate cellular targets other than STAT92E[9].

To investigate whether disruption of heterochromatin induced by Hop-activation[7] is mediated by STAT92E, we examined the effects of reducing *stat92E*$^{+}$ dosage on heterochromatic gene silencing, which can be measured by position-effect variegation (PEV)[12]. As shown previously[7], Hop gain- and loss-of-function mutations suppress and

[2] Correspondence should be addressed to W.X.L. (willis_li@urmc.rochester.edu). .

AUTHOR CONTRIBUTIONS W. X. L. conceived and designed the experiments; S. S., K. L., D. G., S. J. L., P. D. and S.-J. Y. performed the experiments and analysed the data; W. X. L. wrote the paper.

Note: Supplementary Information is available on the Nature Cell Biology website.

enhance PEV, respectively (Fig. 1). We found that reducing *stat92E*$^{+}$ dosage had the opposite effect of reducing Hop and strongly suppressed PEV, causing marked derepression of *white*$^{+}$ in two independent variegated lines *DX1* and *In(1)w*^{m4}, resulting in a substantial increase in red eye-pigmentation (Fig. 1a, c, d–k). Heterozygosity of *stat92E* did not affect expression in a control *P[white*$^{+}$*]* (*6–2 mini-white*$^{+}$) element, which does not induce heterochromatin formation (Fig. 1b, c) or the *white*$^{+}$ gene in its original locus (data not shown; also see ref. 7), suggesting that *P[white*$^{+}$*]* or *white*$^{+}$ is not simply a transcriptional target of STAT92E. Thus, in contrast to Hop, which counteracts heterochromatic gene silencing[7], STAT92E seems to promote this silencing process.

We next examined the epistatic relationship between HP1 and STAT92E (Fig. 1d–k). HP1, encoded by *Su(var)205*, is a constitutive component of heterochromatin and is essential for heterochromatic gene silencing[12,13]. Consistent with the results described above, we found that increasing *stat92E*$^{+}$ dosage by a chromosomal duplication (referred to as 3 × s*tat92E*$^{+}$, Fig. 1f) or a *stat92E*$^{+}$ transgene (Supplementary Information, Fig. S1) enhanced heterochromatic gene silencing, resulting in complete silencing of the variegated *white*$^{+}$ gene. This effect was antagonized, however, by reducing *HP1*$^{+}$ gene dosage (Fig. 1i). It was also evident that the effect of halving *HP1*$^{+}$ gene dosage on derepression of the silenced *white*$^{+}$ gene was strongly opposed by the presence of 3 × *stat92E*$^{+}$ (compare Fig. 1g with 1i). Thus, increasing STAT92E levels promotes gene silencing even when HP1 levels are reduced. Consistent with previous reports[14], increasing HP1 levels by expression of an *hsp70–HP1*$^{+}$ transgene promoted heterochromatin formation, as shown by increased variegation (Fig. 1j). We found that halving *stat92E*$^{+}$ gene dosage counterbalanced the effects of increased HP1, allowing increased *white*$^{+}$ expression (Fig. 1k). However, expression levels of *white*$^{+}$ in *hsp70–HP1*$^{+/-}$;*stat92E*$^{+/-}$ double-heterozygous flies were much lower that those in *stat92E*$^{+/-}$ flies (compare Fig. 1e with 1k), suggesting that increasing HP1 levels also antagonizes the effects of reducing *stat92E*$^{+}$ dosage. Thus, STAT92E and HP1 are interdependent and both required for heterochromatic gene silencing.

We next investigated the requirement for STAT92E in heterochromatin formation by genetic mosaic analyses (see Methods) using HP1 and dimethylated histone H3mK9 as markers in larval salivary glands[7,13]. We found that clonal overexpression of *stat92E*$^{+}$ resulted in higher levels of heterochromatin (H3mK9 and HP1 accumulation), compared with neighbouring wild-type cells (Fig. 2a, b). An increase in the size of the HP1 foci was also found in cells overexpressing a STAT92E–GFP fusion protein (see below). Conversely, in *stat92E*$^{-/-}$ cells, heterochromatin levels, as characterized by HP1 foci, were markedly reduced, compared with neighbouring wild-type cells (Fig. 2c). Notably, the effects of STAT92E overexpression were opposite to those of JAK overactivation on heterochromatin shown previously[7], consistent with the opposite effects we observed on PEV. Thus, STAT92E levels seem to be important for heterochromatin formation or stability.

To further confirm that STAT92E is required for HP1 localization on heterochromatin, we performed chromatin immunoprecipitation (ChIP) using an anti-HP1 antibody before and after *stat92E* knockdown by RNAi in *Drosophila* S2 cells. We chose the transposable element *1360* as a heterochromatin marker to detect the co-immunoprecipitated heterochromatin. *1360* is a repetitive sequence found most abundantly in constitutive heterochromatin regions of all *Drosophila* chromosomes and is believed to be essential for initiating heterochromatin formation[15,16]. Enrichment of HP1 binding to *1360* sequences has been detected previously by ChIP[17]. We found that association of HP1 with *1360* was significantly reduced following *stat92E* RNAi knockdown (Fig. 2d). Thus, STAT92E is essential for the association of HP1 with heterochromatin.

To investigate whether changing STAT92E levels alters HP1 localization in general, we examined additional developmental contexts. First, HP1 localization in heterochromatin can be observed in cellularization-stage (nuclear cycle 14) embryos as foci enriched at the apical region of elongated wild-type nuclei[13,18,19] (Fig. 2e). This pattern of HP1 distribution, however, was absent in mutant embryos lacking maternal *stat92E*$^{+}$ (referred to as *stat92E*$^{mat-}$ embryos; see Methods; Fig. 2f). In these *stat92E*$^{mat-}$ embryos, HP1 protein assumed a punctate and clustered distribution that was no longer restricted to the apical heterochromatin, whereas there were no detectable changes in the total levels of HP1 (compare Fig. 2e with 2f). This is consistent with the notion that STAT92E is required for HP1 localization in centromeric heterochromatin. Second, we examined *stat92E* mutant clones in imaginal discs. The small size of imaginal disc cells does not allow examination of HP1 sub-nuclear distribution, but does allow assessment of total HP1 levels. We found no detectable changes in HP1 levels in *stat92E*$^{-/-}$ imaginal disc cells, compared with neighbouring wild-type cells (Supplementary Information, Fig. S2), suggesting that loss of STAT92E does not immediately cause a substantial reduction in HP1 protein levels. However, long-term loss of s*tat92E*$^{+}$ indeed reduced HP1 levels (Supplementary Information, Fig. S3), suggesting that HP1 transcription may be regulated directly or indirectly by STAT92E. Finally, we examined heterochromatin by performing blots of total protein from embryo extracts. We found that H3mK9 levels were increased significantly in embryos that overexpressed STAT92E and decreased in *stat92E*$^{mat-}$ embryos, whereas HP1 levels were not changed and moderately reduced, respectively (Fig. 2g). These results indicate that, although the canonical JAK/STAT pathway may regulate HP1 transcription, both loss of STAT92E and overactivation of JAK cause HP1 delocalization and overall loss of H3mK9.

The observation that loss of *stat92E*$^{+}$ is equivalent to JAK overactivation and that increasing STAT92E levels has similar effects to loss of *hop*$^{+}$ on heterochromatin formation seemed paradoxical, as JAK activates STAT in the canonical JAK/STAT pathway[3,4]. To understand how STAT92E levels affect heterochromatin formation, we examined STAT92E protein localization by immunostaining with an anti-STAT92E antibody (see Supplementary Information, Figs S4, S6 for specificity). We found that STAT92E was localized mainly in the nucleus in discrete patterns, with the highest levels colocalizing with the HP1 foci (Fig. 3a). Interestingly, it has been shown that unphosphorylated mammalian STAT3 is localized predominantly in the nucleus[20], despite the conventional view that it should be in the cytoplasm. STAT92E colocalization with HP1 in heterochromatin regions was also detected in larval fat bodies or using a different anti-STAT92E antibody (data not shown), or in glands overexpressing a STAT92E–GFP transgene, or by ChIP with S2 cells (see below), indicating that STAT92E is indeed localized in heterochromatin. Nuclear localization of STAT92E–GFP is also evident in unstimulated S2 cells[21]. Moreover, staining of squashed polytene chromosomes from wild-type salivary glands indicated that STAT92E and HP1 colocalize in several regions of heterochromatin, including the chromocentre and telomere (Fig. 3b, c). These results suggest that a significant amount of STAT92E is normally localized on heterochromatin.

As STAT92E colocalizes with HP1, we performed co-immunoprecipitation studies to explore the possibility that STAT92E may interact physically with HP1. Indeed, we found that bacterially expressed GST–HP1 can pull down the endogenous STAT92E from embryo extracts (Fig. 3d), and that HP1 and STAT92E co-immunoprecipitate when transfected in S2 cells (Fig. 3e, lane 4). STAT92E contains a perfect and an imperfect HP1-binding sequence motif PVL[22] (Fig. 3e). We found that mutations of only one or the other site had minimal effects on STAT92E–HP1 binding (Fig. 3e, lanes 5, 6). However, mutations of both sites abolished the STAT92E–HP1 interaction (Fig. 3e, lane 7), suggesting that either of the two sites may be sufficient to mediate STAT92E binding to HP1. Moreover, we found that

endogenous HP1 can co-immunoprecipitate with STAT92E (Fig. 3f, left). Despite the presence of higher levels of both HP1 and STAT92E proteins in *hop-*$^{Tum-l/+}$ embryos, less HP1 was co-immunoprecipitated with STAT92E from these embryos (Fig. 3f). This suggests that unphosphorylated STAT92E binds to HP1, as the ratio of unphosphorylated-to-phosphorylated STAT92E levels was lower in *hop*$^{Tum-l/+}$ than in wild-type embryos (caused by increased STAT92E phosphorylation). Finally, increasing STAT92E phosphorylation, by co-transfecting Hop, reduced the amount of HP1 co-immunoprecipitated with transfected STAT92E (Fig. 3g). These results suggest that unphosphorylated STAT92E can associate with HP1.

We next determined whether the heterochromatin-associated STAT92E is 'active' (that is, tyrosine-phosphorylated) by staining with an anti-phospho-STAT92E antibody[23] (see Supplementary Information, Figs S4, S6 for specificity). Compared with total STAT92E, phosphorylated STAT92E seemed to be distributed more uniformly in the nucleus and did not colocalize with HP1 (Fig. 4a). Moreover, we examined squashed polytene chromosomes from larvae expressing STAT92E–GFP by immunostaining and found that STAT92E–GFP was colocalized either with pSTAT92E or HP1 signals, but rarely with both (Fig. 4b). These results indicate that it is the unphosphorylated form of STAT92E that colocalizes with HP1 on heterochromatin.

To investigate how STAT92E activation by phosphorylation leads to heterochromatin destabilization, we examined STAT92E–GFP and HP1 localization in *ex vivo* cultured salivary glands at different times after stimulating STAT92E phosphorylation with pervanadate (H_2O_2/vanadate), which potently and rapidly increases STAT92E phosphorylation (Supplementary Information, Fig. S6a)[23–25]. Before stimulation, STAT92E–GFP was localized in both cytoplasm and nucleus, with the nuclear portion mostly colocalized with HP1 (Fig. 4c). The higher levels of STAT92E–GFP than endogenous STAT92E in the cytoplasm (compare Fig. 4c with Fig. 3a) may be caused by transgene overexpression. At 20 min post-stimulation, the nuclear STAT92E–GFP was enriched, due to entry of the cytoplasmic protein, and was not colocalized with HP1 (Fig. 4c). This pattern of STAT92E–GFP resembles that of phosphorylated STAT92E (Fig. 4a). We suggest that the change in STAT92E–GFP distribution is caused by nuclear STAT92E–GFP moving away from heterochromatin and cytoplasmic STAT92E–GFP moving into the nucleus following phosphorylation. At 60 min post-stimulation, STAT92E–GFP was mostly bound to euchromatic chromosomes in distinct bands and HP1 had diffused from heterochromatin (Fig. 4c). When an unphosphorylatable mutant *stat92E*^{Y704F}–GFP was overexpressed, however, pervanadate treatment did not cause complete HP1 dispersal and STAT92E^{Y704F}–GFP remained colocalized with HP1 (Fig. 4c). Thus, STAT92E dispersal precedes, and is required for, HP1 displacement from heterochromatin. This conclusion is consistent with observations of HP1 and STAT92E distribution in *hop*$^{Tum-l}$ mutant larval salivary glands (Supplementary Information, Fig. S5). It thus seems that unphosphorylated STAT92E is associated with heterochromatin and phosphorylation causes STAT92E dispersal and translocation to euchromatic regions, presumably binding to cognate promoters.

To confirm this observation, we carried out ChIP experiments in *Drosophila* S2 cells to determine the effects of pervanadate treatment on the abundance of *1360* (heterochromatin) and *stat92E* (target gene) promoter sequences in ChIP, using an anti-STAT92E antibody. Indeed, we found enrichment of *1360* sequences in STAT92E–chromatin complexes before, but not after, treatment with pervanadate (Fig. 4d). The same treatment caused enrichment of phosphorylated STAT92E in the promoter of *stat92E* itself (Fig. 4d).

To investigate whether STAT92E activation could affect heterochromatin indirectly by transcriptionally inducing other genes, we blocked protein synthesis by treating salivary gland with cycloheximide before pervanadate stimulation. We found that cycloheximide treatment did not prevent pervanadate-induced HP1 dispersal (Fig. 5a), but rather, accelerated heterochromatin loss (Fig. 5b). This suggests that heterochromatin destabilization induced by STAT92E activation does not require synthesis of new protein and therefore, cannot be mediated by induction of STAT92E transcription targets.

To further explore the consequences of cycloheximide and pervanadate treatment on STAT92E activation and heterochromatin stability, we examined total protein blots of S2 cell extracts at different times after drug treatment. STAT92E phosphorylation (activation) was evident 5 min after pervanadate treatment and reached a maximum at 1 h in the absence of cycloheximide treatment, but continued to increase in the presence of cycloheximide (Fig. 5b; Supplementary Information, Fig. S6a). The increase in phosphorylated STAT92E levels occurred at the expense of unphosphorylated STAT92E, which was most evident when synthesis of new protein was blocked (Fig. 5b, second panel, lower band), such that after 4 h of drug treatment, unphosphorylated STAT92E levels were significantly reduced (Fig. 5b, second panel, lower band, lane 9). Drug treatment did not significantly affect HP1 levels (Fig. 5b) and cycloheximide treatment alone had no effects on HP1 localization (Fig. 5a), H3mK9 or STAT92E levels or its phosphorylation status (Supplementary Information, Fig. S6b). However, a decrease in the heterochromatin marker H3mK9 was detected 2 h after combined pervanadate and cycloheximide treatment (Fig. 5b).

These results suggest that, in the presence of cycloheximide, pervanadate causes a greater increase in phosphorylated STAT92E levels and a greater decrease in unphosphorylated STAT92E levels, presumably caused by a lack of both positive and negative feedback mechanisms. The negative feedback on STAT activation is mediated by induction of inhibitors such as SOCS36E and PTP61F, which reduce pSTAT92E levels, and the positive feedback by STAT92E autoregulation, which increases STAT92E levels[10]. Both feedback mechanisms require new protein synthesis, which was blocked by cycloheximide. The resultant loss of unphosphorylated STAT92E after combined drug treatment would thus lead to accelerated heterochromatin destabilization. Taken together, these results suggest that activation of STAT92E by phosphorylation causes STAT92E dispersal, leading to HP1 displacement and heterochromatin destruction in a transcription-independent manner (Fig. 5c).

The results of these genetic and biochemical studies suggest a model in which at least a portion of unphosphorylated STAT is normally localized in heterochromatin, where STAT activation causes its diffusion from heterochromatin and relocalization to euchromatin, leading to HP1 dispersal and heterochromatin destabilization (Fig. 5c). Our results, however, do not rule out the possibility that activation of JAK reduces methylation of histone H3mK9 through a STAT-independent mechanism. We envision that under physiological conditions, a low-intensity signal may be sufficient for activating specific STAT target genes without affecting heterochromatin, whereas high intensity or persistent activation of JAK/STAT may bring about widespread heterochromatin destruction. It remains to be determined whether JAK enters the nucleus to phosphorylate STAT or whether the redistribution of unphosphorylated nuclear STAT is a result of an altered equilibrium between nuclear and cytoplasmic or phosphorylated and unphosphorylated STAT in response to JAK activation.

METHODS

Fly stocks and genetics

All crosses were carried out at 25°C on standard cornmeal/agar medium, unless otherwise specified. Fly stocks of *hop*$^{Tum-l}$, *stat92E*^{6346}, *Su(var)205*^{05}, *In(1)w*^{m4}, *Dp(3;3)MRS/+*, *Dp(3;3)M95A[+]13*, *FRT*^{82B} *ubiq–GFP*, *FRT*^{82B} *Gal80*, *hemese–Gal4*, *Nanos–Gal4* and *hsp70–flp; Act5C>y*$^{+}$*>Gal4 UAS–GFP* were from the Bloomington *Drosophila* Stock Center. Fly stocks of *DX1* and *6–2* mini-*white*$^{+}$ (J. Birchler, University of Missouri), *hsp70–HP1* (L. Wallrath, University of Iowa), *UAS–stat92E–EGFP* and *UAS–stat92E*^{Y704F}*–EGFP* (M. Zeidler, University of Sheffied) and *UAS–stat92E* (S. Hou, National Cancer Institute) were gifts.

To express *UAS–stat92E*$^{+}$ in random clones, *hsp70–flp;Act5C>y*$^{+}$*>Gal4 UAS–GFP* flies were crossed with *UAS–stat92E*$^{+}$ flies. To generate *stat92E* loss-of-function clones, we crossed *hsp70–flp; FRT*^{82B} *stat92E*^{6346}*/TM3* females with males of *hsp70–flp; FRT*^{82B} *ubiq–GFP* (for clones in imaginal discs), or *Act5C>y*$^{+}$*>Gal4; FRT*^{82B} *Gal80* (for GFP^{+} clones in salivary glands), or *hsp70–Flp; FRT*^{82B} *[ovo*^{D1}*, w*$^{+}$*]/TM3* (for clones in the female germ-line). The progeny were heat-shocked at 37°C for 2 h in late-embryo (for salivary gland clones) or early-larval stages and allowed to develop at 25°C until examination.

Antibodies, drug treatment, imaging and eye-pigmentation measurement

Mouse monoclonal anti-HP1 (C1A9; 1:200, Developmental Hybridoma Bank), rabbit anti-H3(di)mK9 (07–212, 1:200, Upstate Biotechnology), goat anti-STAT92E (sc-15708; affinity purified against the amino-terminus of STAT92E, 1:200, Santa Cruz), rat anti-STAT92E (1:500)[24] and anti-pSTAT92E (1:1,000, Cell Signaling Technology) were used as primary antibodies and fluorescent secondary antibodies (1:250; Molecular Probes) were used in whole-mount immunostaining. Stained tissues were photographed with a Leica confocal microscope. Images were cropped and minimally processed with Adobe Photoshop 7.0.

To stimulate JAK/STAT activation in S2 cells, 2 mM H_2O_2 and 1 mM sodium vanadate (final concentrations; Sigma) were added for 30 min before collection for ChIP experiments or as indicated. For salivary gland *ex vivo* culture, the final concentrations were 5 mM H_2O_2 and 0.5 mM vanadate. Alternatively, salivary glands were pretreated with cycloheximide (0.1 mg ml^{-1}; Sigma) for 1 h or as indicated.

To measure eye pigmentation, the heads of 40 female flies (2–3 days old, raised at 25°C) of each genotype were homogenized in methanol (1 ml, acidified with 0.1% HCl). Eye pigmentation was represented as the absorbance of the supernatant at 480 nm.

Cell culture, oligonucleotides and plasmids

V5–STAT92E and Hop expression plasmids in pMT vector were gifts from S. Hou. Oligonucleotides used to amplify the *1360* transposon (forward: TGTATCGTTTTTAAAAAATTGTCAG; reverse: GTGGACCTGTAATATATGCTCT) were as described[17]. A 500-bp *stat92E* cDNA fragment was amplified by T7 promoter attached to PCR primers (forward: GAAT TAATACGACTCACTATAGGGAGACTTGCCCAAAACTACAGTTAC; reverse: GAATTAATACGACTCACTATAGGGAGACGACTGTGGGTGGATTGTT) and used for *stat92E* RNAi synthesis by *in vitro* transcription with the Fermentas T7 RNA transcription kit, according to the manufacturer's instruction.

Drosophila Schneider L2 (S2) cells were cultured at 25°C in *Drosophila* serum-free medium (Invitrogen) supplemented with 10% fetal bovine serum (FBS, Invitrogen) and 0.5×

antibiotic-antimycotic (Invitrogen) solution. Cells were cultured at 2.5×10^6 ml^{-1} before transfection, which was performed with Cellfectin (Invitrogen), according to the manufacturer's instructions. Copper sulphate (Sigma) was added to the medium 16 h after transfection, at a final concentration of 0.5 mM, and cells were collected 48 h of after induction. S2 cells were collected in cell lysis buffer (Cell Signaling Technology). For RNAi treatment, cells were grown in serum-free medium for 12 h before addition of dsRNA (15 μg ml^{-1}). Cells were grown for another 4 days before processing.

ChIP

Analysis was performed according to standard protocols (see Supplementary Information) with the following modifications: 1×10^7 confluent S2 cells were cross-linked with 1% formaldehyde. The cell lysate was sonicated to produce DNA fragments of 500–1000 bps. Chromatin (25 μg; determined by A_{260nm}) was pre-cleared with protein G beads and then precipitated with primary antibody (5 μg in 1 ml total volume) overnight at 4°C. Following purification with protein G beads, samples were heated at 65°C for 5 h to reverse cross-linking. Genomic DNA was purified with QIAquick (Qiagen) and amplified with specific PCR primers.

Supplementary Material

Refer to Web version on PubMed Central for supplementary material.

Acknowledgments

We thank J. Birchler, S. Elgin, S. Hou, L. Wallrath, M. Zeidler, G. Reuter, the Developmental Hybridoma Bank (Iowa), the Bloomington *Drosophila* Stock Center for *Drosophila* strains and reagents and H. Land and D. Bohmann for helpful comments on the manuscript. This study was supported, in part, by grants from the National Institutes of Health (R01GM65774; R01GM077046), an American Cancer Society Research Scholar Grant (RSG-06-196-01-TBE) and a Leukemia & Lymphoma Society Research Scholar Grant (1087-08) to W.X.L.

References

1. Bromberg J. Stat proteins and oncogenesis. J. Clin. Invest. 2002; 109:1139–1142. [PubMed: 11994401]
2. Yu H, Jove R. The STATs of cancer – new molecular targets come of age. Nature Rev. Cancer. 2004; 4:97–105. [PubMed: 14964307]
3. Aaronson DS, Horvath CM. A road map for those who know JAK-STAT. Science. 2002; 296:1653–1655. [PubMed: 12040185]
4. Darnell JE Jr, Kerr IM, Stark GR. Jak-STAT pathways and transcriptional activation in response to IFNs and other extracellular signaling proteins. Science. 1994; 264:1415–1421. [PubMed: 8197455]
5. Harrison DA, Binari R, Nahreini TS, Gilman M, Perrimon N. Activation of a *Drosophila* Janus kinase (JAK) causes hematopoietic neoplasia and developmental defects. EMBO J. 1995; 14:2857–2865. [PubMed: 7796812]
6. Luo H, Hanratty WP, Dearolf CR. An amino acid substitution in the *Drosophila* hopTum-l Jak kinase causes leukemia-like hematopoietic defects. EMBO J. 1995; 14:1412–1420. [PubMed: 7729418]
7. Shi S, et al. JAK signaling globally counteracts heterochromatic gene silencing. Nature Genet. 2006; 38:1071–1076. [PubMed: 16892059]
8. Hanratty WP, Dearolf CR. The *Drosophila* Tumorous-lethal hematopoietic oncogene is a dominant mutation in the hopscotch locus. Mol. Gen. Genet. 1993; 238:33–37. [PubMed: 8479437]
9. Betz A, Darnell JE Jr. A Hopscotch-chromatin connection. Nature Genet. 2006; 38:977–979. [PubMed: 16941005]
10. Arbouzova NI, Zeidler MP. JAK/STAT signalling in *Drosophila*: insights into conserved regulatory and cellular functions. Development. 2006; 133:2605–2616. [PubMed: 16794031]

11. Hou SX, Zheng Z, Chen X, Perrimon N. The Jak/STAT pathway in model organisms. Emerging roles in cell movement. Dev. Cell. 2002; 3:765–778. [PubMed: 12479803]
12. Grewal SI, Elgin SC. Heterochromatin: new possibilities for the inheritance of structure. Curr. Opin. Genet. Dev. 2002; 12:178–187. [PubMed: 11893491]
13. James TC, et al. Distribution patterns of HP1, a heterochromatin-associated nonhistone chromosomal protein of *Drosophila*. Eur. J. Cell Biol. 1989; 50:170–180. [PubMed: 2515059]
14. Li Y, Danzer JR, Alvarez P, Belmont AS, Wallrath LL. Effects of tethering HP1 to euchromatic regions of the *Drosophila* genome. Development. 2003; 130:1817–1824. [PubMed: 12642487]
15. Kaminker JS, et al. The transposable elements of the *Drosophila melanogaster* euchromatin: a genomics perspective. Genome Biol. 2002; 3:0084.1–0084.20.
16. Sun FL, et al. *cis*-Acting determinants of heterochromatin formation on *Drosophila melanogaster* chromosome four. Mol. Cell Biol. 2004; 24:8210–8220. [PubMed: 15340080]
17. De Lucia F, Ni JQ, Vaillant C, Sun FL. HP1 modulates the transcription of cell-cycle regulators in *Drosophila melanogaster*. Nucleic Acids Res. 2005; 33:2852–2858. [PubMed: 15905474]
18. Kellum R, Raff JW, Alberts BM. Heterochromatin protein 1 distribution during development and during the cell cycle in *Drosophila* embryos. J. Cell Sci. 1995; 108:1407–1418. [PubMed: 7615662]
19. Shareef MM, et al. *Drosophila* heterochromatin protein 1 (HP1)/origin recognition complex (ORC) protein is associated with HP1 and ORC and functions in heterochromatin-induced silencing. Mol. Biol. Cell. 2001; 12:1671–1685. [PubMed: 11408576]
20. Liu L, McBride KM, Reich NC. STAT3 nuclear import is independent of tyrosine phosphorylation and mediated by importin-α3. Proc. Natl Acad. Sci. USA. 2005; 102:8150–8155. [PubMed: 15919823]
21. Karsten P, Plischke I, Perrimon N, Zeidler MP. Mutational analysis reveals separable DNA binding and *trans*-activation of *Drosophila* STAT92E. Cell Signal. 2006; 18:819–829. [PubMed: 16129580]
22. Thiru A, et al. Structural basis of HP1/PXVXL motif peptide interactions and HP1 localisation to heterochromatin. EMBO J. 2004; 23:489–499. [PubMed: 14765118]
23. Li J, et al. Patterns and functions of STAT activation during *Drosophila* embryogenesis. Mech. Dev. 2003; 120:1455–1468. [PubMed: 14654218]
24. Li WX, Agaisse H, Mathey-Prevot B, Perrimon N. Differential requirement for STAT by gain-of-function and wild-type receptor tyrosine kinase Torso in *Drosophila*. Development. 2002; 129:4241–4248. [PubMed: 12183376]
25. Sweitzer SM, Calvo S, Kraus MH, Finbloom DS, Larner AC. Characterization of a Stat-like DNA binding activity in *Drosophila melanogaster*. J. Biol. Chem. 1995; 270:16510–16513. [PubMed: 7622453]
26. Dorer DR, Henikoff S. Expansions of transgene repeats cause heterochromatin formation and gene silencing in *Drosophila*. Cell. 1994; 77:993–1002. [PubMed: 8020105]
27. Ronsseray S, Boivin A, Anxolabehere D. P-Element repression in *Drosophila melanogaster* by variegating clusters of P-lacZ-white transgenes. Genetics. 2001; 159:1631–1642. [PubMed: 11779802]

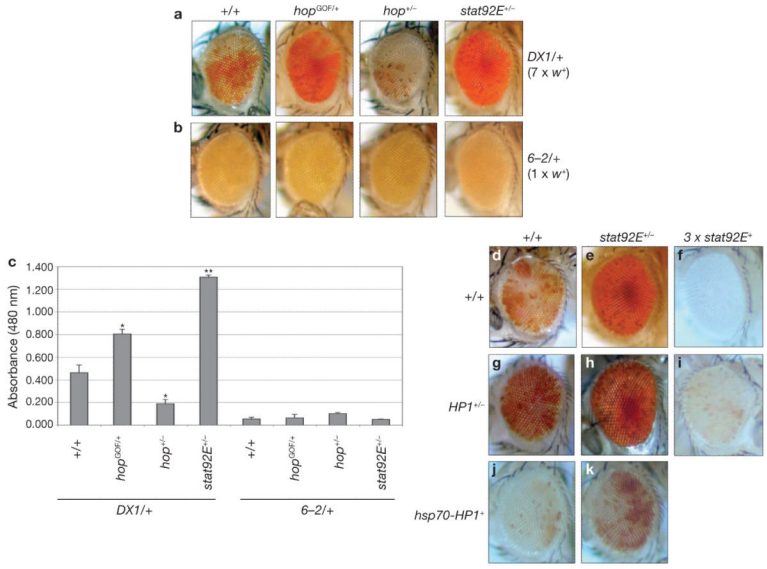

Figure 1.

STAT92E is required for heterochromatic gene silencing. (**a**–**c**) Effects of mutations in *hop* and *stat92E* on *white*$^{+}$ variegation induced by transgene repeats, *DX1* (**a**) or a control transgene (**b**) are shown as changes in red eye-pigmentation in representative images. *DX1* consists of seven tandem copies of a *P[white*$^{+}$*]* reporter transgene inserted in a euchromatic region, which induce heterochromatin formation at the insertion locus[26]. *In(1)w*^{m4} is caused by X chromosomal inversion, juxtaposing the *white*$^{+}$ gene to centromeric heterochromatin[12]. (**c**) Red eye-pigment levels were determined by measuring absorbance at a wavelength of 480 nm. Data are mean ± s. d, $^{**}P < 0.001$ when compared with +/+ control, Student's *t*-test ($n = 40$ for each group). *6–2* is a single *P[white*$^{+}$*]* element inserted at the same chromosomal location as *DX1* but that does not induce heterochromatin formation[26,27]. (**d**–**k**) Effects of altering dosages of *stat92E*$^{+}$ and/or *HP1*$^{+}$ on *white*$^{+}$ variegation induced by chromosomal inversion (*In(1)w*^{m4}) are shown as changes in red eye-pigmentation in representative images. (**d**) *In(1)w*^{m4} in otherwise wild-type background. Note increased *white*$^{+}$ expression (more red pigments) in *stat92E* (**e**, **h**, **k**) or *HP1* heterozygotes (**g**–**i**) and decreased *white*$^{+}$ expression when *stat92E*$^{+}$ (**f**, **i**) or *HP1*$^{+}$ is overexpressed (**j**, **k**). The combination of *hsp70–HP1*$^{+}$ and 3 × *stat92E*$^{+}$ was not viable. Flies bearing *hsp70–HP1*$^{+}$ were raised at 29°C. All others were raised at 25°C. All genotypes are in *In(1)*$^{wm4/+}$ or *w*$^{-/-}$ backgrounds. (*hop*^{GOF}=*hop*$^{Tum-l}$, *hop*$^{-}$=*hop*^{3}, *stat92E*$^{-}$=*stat92E*^{6346}, *HP1*$^{-}$=*Su(var)205*^{05}, 3 × *stat92E*$^{+}$=*Dp(3;3)MRS/+*). Similar results were observed when another chromosomal duplication, *Dp(3;3)M95A[+]13*, that duplicates *stat92E*$^{+}$ was used (data not shown), or by a *stat92E*$^{+}$ transgene (Supplementary Information, Fig. S1).

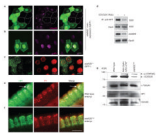

Figure 2.

STAT92E levels control heterochromatin abundance and HP1 localization. (**a**, **b**) Third-instar salivary glands overexpressing *stat92E*$^{+}$ in random cells marked with GFP (green) and stained with anti-H3mK9 (magenta in **a**) or anti-HP1 (magenta in **b**) are shown partially. Note the increased levels of H3mK9 or HP1 in GFP^{+} cells, compared with GFP^{-} cells (four GFP^{-} cells are outlined). (**c**) A third-instar salivary gland containing *stat92E*$^{-/-}$ cells marked with GFP (green) and stained with anti-HP1 (red) is shown partially. Note the lack of HP1 foci in the GFP^{+} cells. (**d**) Enrichment of HP1 on heterochromatin was detected by ChIP using an anti-HP1 antibody and PCR primers that amplify the *1360* transposon element (heterochromatin). Note the marked reduction in HP1 association with *1360* sequences in the STAT92E RNAi-depleted sample (lane 2), compared with the control (lane 1). (**e**, **f**) Cellular blastoderm-stage embryos stained with anti-HP1 (green) and propidium iodide (PI; red) to show DNA. Part of the cortical cell layer is shown. Note the concentrated HP1-staining at the apical region of the wild-type embryo (arrow in **e**), which is absent in the *stat92E*$^{mat-}$ embryo (**f**). (**g**) Total protein extracts from 0–12 hold embryos of wild-type (lane 1), *Nanos–Gal4* × *UAS–stat92E*$^{+}$ (lane 2) and *stat92E*$^{mat-}$ females (lane 3) were subjected to SDS–PAGE and blotted sequentially with anti-STAT92E and anti-α-tubulin antibodies (for full-length gel, see Supplementary Information, Fig. S7), or with anti-H3mK9 and anti-HP1 antibodies, respectively. The membrane was stripped between blots. Note the correlation between H3mK9 and STAT92E levels. Scale bars, 10 μm.

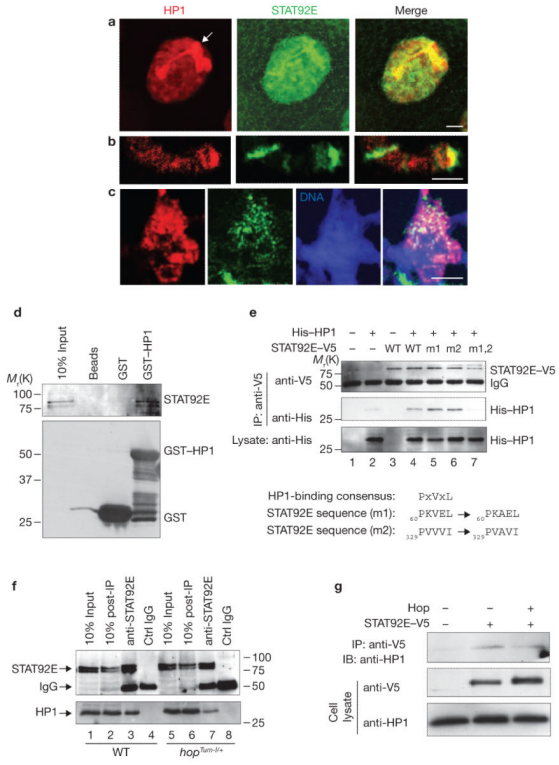

Figure 3.

STAT92E colocalizes and physically associates with HP1. (**a**–**c**) Third-instar wild-type salivary glands were stained with anti-HP1 (red) and anti-STAT92E (green) antibodies in whole-mount tissues or squashed polytene chromosomes. Representative giant nuclei and squashed chromosomes are shown. (**a**) In wild-type larvae, the HP1 foci in the salivary gland nuclei, which mark heterochromatin, colocalize with STAT92E. In squashed chromosomes, STAT92E and HP1 colocalization is shown in the telomere (**b**) and chromocentre (**c**). (**d**) *Drosophila* embryo extracts were incubated with bacterially expressed GST–HP1, which was then purified by glutathione beads, subjected to SDS–PAGE and blotted with an anti-STAT92E antibody. (**e**) *Drosophila* S2 cells transfected with or without STAT92E–V5 variants or His–HP1 were immunoprecipitated with an anti-V5 antibody and subjected to SDS–PAGE. The associated His–HP1 was detected with an anti-His antibody. Note the double-mutant STAT92E–V5 (lane 7) was unable to bind to HP1. The HP1-binding consensus motif, the two sequences present in STAT92E and the mutated sequences are shown under the blots. (**f**) Embryo extracts were immunoprecipitated with an anti-STAT92E antibody, subjected to SDS–PAGE and blotted with anti-HP1. Note that a greater amount of the endogenous HP1 was co-immunoprecipitated with endogenous STAT92E from wild-type than $hop^{Tum-l/+}$ embryos. Also note that depleting STAT92E using an antibody did not seem to affect HP1 levels in the lysate (lanes 2, 6), suggesting that perhaps only a small portion of HP1 is normally associated with STAT92E. (**g**) S2 cells transfected with or without STAT92E–V5 or Hop (lane 3) were immunoprecipitated with anti-V5 and subjected to SDS–PAGE. The associated endogenous HP1 was detected with an anti-HP1 antibody. Note that HP1 is co-immunoprecipitated with STAT92E–V5 (lane 2) and a reduced amount of HP1 is detected in the presence of Hop (lane 3). Scale bars, 2 μm.

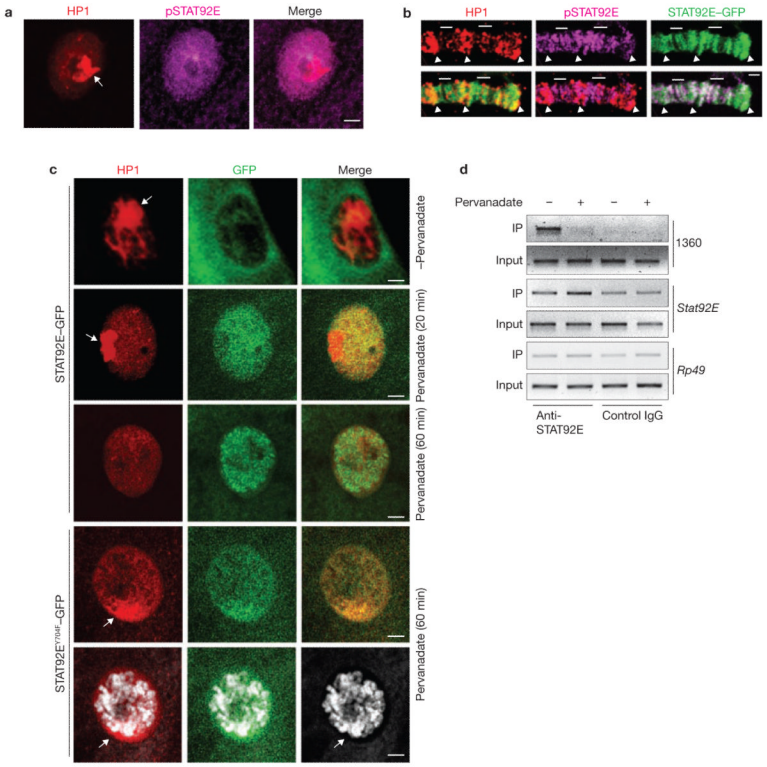

Figure 4.

Only unphosphorylated STAT92E is localized on heterochromatin. (**a**) Wild-type larval salivary gland stained with anti-HP1 and anti-pSTAT92E antibodies. Note that the signals do not overlap. (**b**) In polytene chromosomes from *sgs–Gal4<UAS–stat92E–GFP* larvae, STAT92E–GFP was colocalized with either pSTAT92E (bars) or HP1 (arrowheads) signals. (**c**) Third-instar larval salivary glands expressing UAS–STAT92E–GFP or STAT92E^{Y704F}–GFP (by *arm–Gal4*) were treated with pervanadate *ex vivo*. Distribution of HP1 (red) and STAT92E–GFP or STAT92EY704F–GFP (green) was examined at the indicated time points. Note that following pervanadate stimulation, STAT92E–GFP moves away from heterochromatin (HP1 foci; 20 min) and then binds to chromosomes as distinct bands (60 min), whereas UAS–STAT92E^{Y704F}–GFP remains colocalized with HP1 foci (60 min). DNA was stained with Toto-3. (**d**) Chromatin was immunoprecipitated from S2 cells with an anti-STAT92E antibody (which recognizes both unphosphorylated and phosphorylated STAT92E) before and after pervanadate treatment. Note the enrichment of STAT92E on heterochromatin (*1360*; row 1) and target-gene promoter (*stat92E* itself) before (lane 1) and after (lane 2) pervanadate treatment. The *stat92E* promoter contains multiple STAT92E-binding sites that mediate *stat92E* positive-feedback autoregulation. *Rp49* is a negative control (row 3). A goat anti-human pan SMAD antibody was used as a control IgG for goat anti-STAT92E. Scale bars, 2 μm.

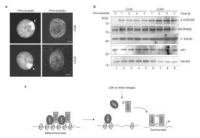

Figure 5.

Protein-synthesis-independent heterochromatin disruption following STAT92E phosphorylation. (**a**) Wild-type salivary glands were cultured with or without cycloheximide (CHX) for 1 h before addition of pervanadate for 1 h *in vitro*. Represented nuclei are shown. Note the disappearance of the HP1 foci in treated cells. (**b**) S2 cells were cultured with or without CHX for 1 h, and then stimulated with pervanadate for the indicated times. Cell extracts were blotted with the indicated antibodies. Note a greater increase in pSTAT92E (phosphorylated) and decrease in STAT92E (unphosphorylated) bands in CHX-treated samples, which is correlated with a greater decrease in H3mK9 levels. (**c**) A model for the role of STAT in heterochromatin stability. Unphosphorylated STAT is localized on heterochromatin in association with HP1. Increasing STAT phosphorylation (by JAK or other tyrosine kinases) reduces the amount of unphosphorylated STAT localized in heterochromatin. This in turn causes HP1 displacement from heterochromatin and heterochromatin instability. Dispersed phosphorylated STAT binds to cognitive sites in euchromatin to induce target-gene expression. Scale bars, 2 μm.